
Sparsity Normalization: Stabilizing the Expected Outputs of Deep Networks

Joonyoung Yi¹, Juhyuk Lee¹, Sung Ju Hwang^{1,2}, Eunho Yang^{1,2}
KAIST¹, AITRICS², South Korea
{joonyoung.yi, sehkmg, sjhwang82, eunhoy}@kaist.ac.kr

Abstract

The learning of deep models, in which a numerous of parameters are superimposed, is known to be a fairly sensitive process and should be carefully done through a combination of several techniques that can help to stabilize it. We introduce an additional challenge that has never been explicitly studied: the heterogeneity of sparsity at the instance level due to missing values or the innate nature of the input distribution. We confirm experimentally on the widely used benchmark datasets that this *variable sparsity problem* makes the output statistics of neurons unstable and makes the learning process more difficult by saturating non-linearities. We also provide the analysis of this phenomenon, and based on our analysis, we present a simple technique to prevent this issue, referred to as Sparsity Normalization (SN). Finally, we show that the performance can be significantly improved with SN on certain popular benchmark datasets, or that similar performance can be achieved with lower capacity. Especially focusing on the collaborative filtering problem where the variable sparsity issue has been completely ignored, we achieve new state-of-the-art results on Movielens 100k and 1M datasets, by simply applying Sparsity Normalization (SN).

1 Introduction

The rapid progress of deep learning in recent years was made possible with availability of large-scale datasets and advancement of computing processors. Not only that, but a variety of learning techniques and deeper understanding of deep learning has enabled more effective learning of challenging models that were previously thought to be difficult to train. The introduction of ReLU [1] alleviated the problem of gradient vanishing, allowing us to build a deeper network with significantly better performances [2, 3]. The introduction of simple but systematic ways to initialize the network has made the learning of the deep models relatively easy [4, 5], and the skip connection methodologies enabled us to build extremely deep networks [6, 7].

Input and hidden layer normalization techniques also have made significant contributions to recent achievements in deep learning. Commonly used input normalization techniques such as min-max normalization and standardization maintain the stability of the statistics of the input layer so that the learning is not biased, thus improving the overall performance. Techniques that normalize hidden layers, such as batch normalization [8] and layer normalization [9], could be considered as a generalized form of input-normalization, with hidden layer as input. Several studies have shown that normalization techniques, by modifying the hidden layer statistics, lead to stable learning and improved performances [10, 11, 12].

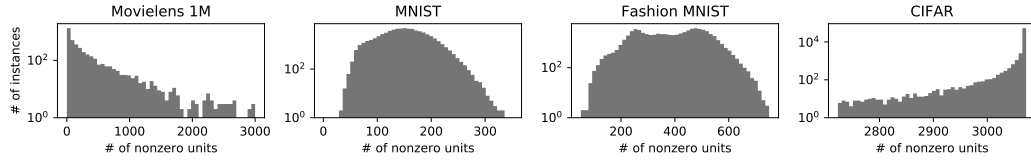


Figure 1: A histogram of the sparsity in Movielens, MNIST, Fashion MNIST, and CIFAR. The x-axis represents the number of nonzero inputs, and the y-axis represents the number of such data instances.

However, these normalization techniques have overlooked the effect of sparsity. In this paper, we focus on our novel finding that when the sparsity varies largely between input instances, the learning can not be done properly due to the variations of the statistics at the output layer. We refer to this problem as the *variable sparsity problem*. Variable sparsity problems are abundant in real-world datasets. For example, electronic health records (EHR) often contain different sets of medical examinations for each patient. Similarly, for collaborative filtering tasks, the user entries could have varying degree of sparsity based on each user’s item experience. In addition to the limitations at the data acquisition stage as above, this phenomenon can arise depending on the distribution of the original value of the feature, even in the datasets for which we may misunderstand as having no heterogeneity of sparsity due to absence of missing values. In the benchmark datasets such as MNIST [13], Fashion MNIST [14], and CIFAR [15], which are recently used as standards in the computer vision tasks, there are a large differences in sparsity levels over data instances (see Figure 1).

For a better understanding of this phenomenon, we first prove that the expected output of a neural network is dependent not only on the input value but also on its *sparsity* under the assumption similar to those in [4, 5]. Based on this analysis, we propose a Sparsity Normalizing (SN) technique as a simple solution to satisfy the conditions in which the expected output of a deep network can remain unchanged with the sparsity level of input.

Although SN is very simple, it is surprisingly effective and can indeed improve the performance by stabilizing the distribution of the network output. Especially, a line of work using deep models for collaborative filtering [16, 17] has completely overlooked this *variable sparsity problem*, and we achieve the state-of-the-art results on Movielens 100k and 1M datasets, by just applying SN on these models. We also apply SN to general regression and classification problems and obtain the improved performances (for UCI, Medical datasets) or at least similar performances with lower network capacity (for MNIST, Fashion MNIST, CIFAR).

In addition, our analysis and SN technique provide a deeper understanding of some phenomena that are temporarily known just empirically. Specifically, variable sparsity problem can provide explanations to the following: 1) the fact that zero imputation of missing data has a negative effect on learning in deep networks, 2) the need of similar form of normalization techniques already used in several popular models such as GCN [18] and Word2Vec [19] 3) the inherent ability of RNN-based models (such as LSTM, GRU) to handle sparsity.

The main contributions of this paper are as follows:

- We present the *variable sparsity problem* where the expected output of a neural network varies largely with respect to input sparsity, leading to unstable learning on instances with varying degree of sparsity. We experimentally show that this problem occur frequently in many datasets.
- We present a solution termed *sparsity normalization (SN)* that can theoretically resolve the *variable sparsity problem* under some strong conditions.
- We validate SN on diverse tasks and show that despite its simplicity, SN can consistently help stabilize the learning process and provide significant performance improvements. Especially, we achieve the state-of-the-art results with SN on collaborative filtering task.

2 Related Works

Output layer stabilization Thus far, several attempts have been made to stabilize the output of deep networks. First, input normalization techniques stabilize the input layer statistics so that the output layer does not change significantly [20, 21]. Hidden layer normalization techniques such as batch normalization [8] and layer normalization [9] leverage hidden layer statistics to solve problems known to interfere with learning such as internal covariance shifts and low Lipschitzness levels [22], thus help stabilizing training of the output layer [10, 11, 12, 23]. Existing normalization techniques tend to normalize all data instances with the global statistics. In our approach, normalization is performed differently for each data instance, contributing to more stable learning.

Handling missing features Imputation approaches are the most popular techniques to handle missing features for stable learning. Using median or mean values of the input is the most straightforward approach for imputation, but it could lead to highly incorrect estimation since they do not take into consideration the characteristics of each data instance [24, 25]. To overcome this limitation, researchers have proposed various ways to learn how to impute missing values for each instance, using autoencoders, GANs, and RNNs [26, 27, 28, 29, 30, 31]. However, these learning-based imputation methods are still limited, since they require learning of additional models and may be prone to overfitting. Some approaches tackle this issue by handling missing values in an end-to-end learning frameworks, but they still require additional parameters for handling missingness [32, 33, 34, 25, 35]. In this work, we propose a simple yet effective approach that does not require additional networks nor increase the network parameters, and can properly handle missingness.

Handling missing values in neural net-based collaborative filtering Handling missing values is a crucial problem in designing neural net-based algorithms for collaborative filtering, since the data domain they deal with usually have extremely high sparsity rates. Some of the most popular datasets for collaborative filtering have less than 5% of observable entries, and the rest are missing. Due to such high sparsity rates, existing approaches that handle missing data do not perform well [36]. [37, 38] attempt to reduce the effects of the high sparsity rates by using matrix factorization, but these are not a fundamental solution to the high rates of sparsity. The most popular means of handling missing in neural net-based collaborative filtering is to use regularization. Several studies, including CF-NADE [17] and AutoRec [16], have used some regularizations such as weight decay to try to tackle the high degree of sparsity [39]. However, the proposed regularization schemes tend to be limited in that they are only applicable to the collaborative filtering problems and ignore the heterogeneity of sparsity at the instance level.

3 Variable Sparsity Problem

This section introduces the *variable sparsity problem* and theoretically demonstrates the conditions under which we experience it. Next, we experimentally confirm with UCI datasets that it actually occurs under more general circumstances.

3.1 Definition and existence analysis

We define the *variable sparsity problem* as follows: the expected value of the output layer of a deep network (over the weight and input distributions) depends on the sparsity (the number of zero values) of the input data and hence we have varying activation values for data instances with similar characteristics under different sparsity levels, which makes the overall training difficult. In this subsection, we show several example cases of the *variable sparsity problem*. Specifically, we show the *variable sparsity problem* under assumptions with increasing generality (**Case 1**) where the activation function is the identity with no bias, (**Case 2**) where the activation function is an affine function, and (**Case 3**) where the activation function is a convex function such as ReLU [1], leaky ReLU [40], ELU[41], or Softplus [42].

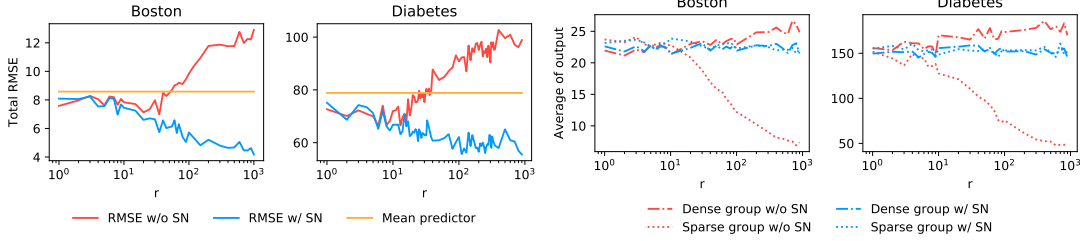


Figure 2: Left two figures shows RMSE in terms of the number of replications r . RMSE of model without SN gets higher than that of the mean predictor (average of outputs over all training data) as r increases. Right two figures show output layer activations of each group.

Here, we summarize the notation for clarity. For L -layer deep networks with non-linearity σ , we use $W^i \in \mathbb{R}^{n_i \times n_{i-1}}$ to denote the weight matrix of i -th layer, $\mathbf{b}^i \in \mathbb{R}^{n_i}$ to denote the bias, $\mathbf{h}^i \in \mathbb{R}^{n_i}$ to denote the activation vector. For simplicity, we use $\mathbf{h}^0 \in \mathbb{R}^{n_0}$ and $\mathbf{h}^L \in \mathbb{R}^{n_L}$ to denote input and output layer, respectively. Then, we have

$$\mathbf{h}^i = \sigma(W^i \mathbf{h}^{i-1} + \mathbf{b}^i), \quad \text{for } i = 1, \dots, L. \quad (1)$$

Our goal in this subsection is to observe the change in \mathbf{h}^L as the sparsity of \mathbf{h}^0 (or input \mathbf{x}) changes. To simplify the discussion, we consider the following assumption:

Assumption 1. (i) Every coordinate of input vector, h_l^0 , is generated by the multiplication of two random variables \tilde{h}_l^0 and m_l where m_l is binary mask indicating missing value and \tilde{h}_l^0 is a (possibly unobserved) feature value. Here, missing mask m_l is MCAR (missing completely at random), with no dependency with other mask variables or their values $\tilde{\mathbf{h}}^0$. All m_l follow some identical distribution with mean μ_m . (ii) The elements of matrix W^i are mutually independent and follow the identical distribution with mean μ_w^i . Similarly, \mathbf{b}^i and $\tilde{\mathbf{h}}^0$ consist of i.i.d. coordinates with mean μ_b^i and μ_x , respectively. (iii) μ_w^i is not zero uniformly over all i .

(i) assumes the simplest missing mechanism. (ii) is similarly defined in [4] and [5]. (iii) may not hold under some initialization strategies, but as the learning progresses, it is very likely to hold.

(Case 1) For simplicity, let us first consider networks without the non-linearity nor the bias term. Theorem 1 shows that the average value of the output layer $E[h_l^L]$ is directly proportional to the expectation of the mask vector μ_m :

Theorem 1. Suppose that activation σ is an identity function and that b_l^i is uniformly fixed as zero under Assumption 1. Then, we have $E[h_l^L] = \prod_{i=1}^L n_{i-1} \mu_w^i \mu_x \mu_m$.

(Case 2) When the activation function is affine but now with a possibly nonzero bias, $E[h_l^L]$ is influenced by μ_m in the following way:

Theorem 2. Suppose that activation σ is an affine function under Assumption 1. Suppose further that $f_i(x)$ is defined as $\sigma(n_{i-1} \mu_w^i x + \mu_b^i)$. Then, $E[h_l^L] = f_L \circ \dots \circ f_1(\mu_x \mu_m)$.

(Case 3) Finally, when the activation function is non-linear but convex, we can show that $E[h_l^L]$ is lower-bounded by some quantity involving μ_m :

Theorem 3. Suppose that σ is a convex function under Assumption 1. Suppose further that $f_i(x)$ is defined as $\sigma(n_{i-1} \mu_w^i x + \mu_b^i)$. Then, $E[h_l^L] \geq f_L \circ \dots \circ f_1(\mu_x \mu_m)$.

If the expected value of the output layer depends on the level of sparsity as in Theorem 1-3, even similar data instances may have a different output values depending on the sparsity, which would hinder the learning process to remain stable.

3.2 Variable sparsity problems on UCI datasets

In this subsection we experimentally show the effect of heterogeneous sparsity using two UCI datasets where Assumption 1 might be violated¹. Toward this, we manipulate the datasets as follows. Instead of injecting a certain probability of sparsity (erasing features independently with this probability) into all data instances as done in [34, 43], we divide data instances into two groups: half of the data with sparsity of 80% (sparse group) and the other half with 20% (dense group). In order to see the effect of absolute gaps in two groups' sparsity levels, we simply copy the input r times to make extended feature vector $\mathbf{x}' \in \mathbb{R}^{r n_0} = [\mathbf{x}^{(1)}; \dots; \mathbf{x}^{(r)}]$ (where $\mathbf{x}^{(j)}$ is j -th identical copy of \mathbf{x}) before the sparsity injection².

The larger the value of r is, the greater the amount of information is given to the network (since the sparsity is injected after feature duplication). As a result, if the networks are trained properly, the test RMSE should be reduced. Surprisingly, however, as shown in Figure 2, the total RMSE (over all sparse and dense groups) increases as r increases. Not only that, as r changes, the expected outputs change differently according to the sparsity level.

4 Sparsity Normalization

In this section, we propose a simple solution to resolve the *variable sparsity problem*. Toward this, we revisit Theorem 2 above to find a way of making expected output independent of input sparsity level. Recalling the notation of $\mathbf{h}^0 = \tilde{\mathbf{h}}^0 \odot \mathbf{m}$ (\odot represents the element-wise product) in Section 3, we find that simply normalizing via $\mathbf{h}_{\text{SN}}^0 = (\tilde{\mathbf{h}}^0 \odot \mathbf{m}) \cdot K / \mu_m$ for any fixed constant K , can correct the dependency on the input sparsity level as follows:

Theorem 4. (*Sparsity Normalization*) *Suppose that activation σ is an affine function under Assumption 1. Suppose further that $f_i(x) = \sigma(n_{i-1}\mu_w^i x + \mu_b^i)$ and replace the input layer using SN, i.e. $\mathbf{h}_{\text{SN}}^0 = (\tilde{\mathbf{h}}^0 \odot \mathbf{m}) \cdot K / \mu_m$ for any fixed constant K . Then, we have $E[h_L^L] = f_L \circ \dots \circ f_1(\mu_x \cdot K)$.*

Theorem 4 shows that with SN, the average activation of the output layer does not depend on μ_m anymore, leading to a constant level of output, regardless of the sparsity. It is instructive to note that it is not trivial to show similar result for SN under **(Case 3)** since $E[\sigma(x)] = \sigma(E[x])$ is not established in this case. However, we show in the experimental section that SN is practically effective even in more general cases. Also in the experiments in Figure 2, we confirm that expected output remains constant with SN (right two figures) and RMSE properly improves as r increases.

While we assume μ_m is fixed as a constant across instances in Assumption 1, we relax this assumption and consider varying μ_m for every input. Then, by maximum likelihood estimation, we can estimate μ_m by $\|\mathbf{h}^0\|_0 / n_0$. Thus, we have $\mathbf{h}_{\text{SN}}^0 = K' \cdot \mathbf{h}^0 / \|\mathbf{h}^0\|_0$ where $K' = n_0 \cdot K$ (See Algorithm 1).

In practice, we use $K' = n_0$ for the extremely deep network with ReLU activation. The reason is that small K' value is likely to make the final activation of a ReLU network zero, which is called dying

¹We deliberately choose two regression tasks in order to make it easy to visualize the output variations. We use zero-one input normalization, ReLU activations with 3 hidden layered MLP and 100 hidden units in each layer. We keep the ratio of training set to valid set to test set as 3:1:1.

²A figure on generating this process is given in the Appendix C.1 for clarity. (see Figure 5)

Table 1: Test RMSE on Movielens 100k, 1M, 10M datasets.

Datasets		Movielens 100k		Movielens 1M		Movielens 10M	
input vector		item vector	user vector	item vector	user vector	item vector	user vector
AutoRec	w/o SN	0.8831 ± 0.0187	0.9343 ± 0.0221	0.8306 ± 0.0018	0.8832 ± 0.0025	0.7807 ± 0.0017	0.8859 ± 0.0014
	w/ SN	0.8822 ± 0.0170	0.9217 ± 0.0217	0.8275 ± 0.0026	0.8738 ± 0.0014	0.7706 ± 0.0023	0.8462 ± 0.0005
CF-NADE	w/o SN	0.8907 ± 0.0201	0.9258 ± 0.0200	0.8398 ± 0.0016	0.8570 ± 0.0045	N/A	0.8113 ± 0.0058
	w/ SN	0.8882 ± 0.0183	0.9200 ± 0.0186	0.8383 ± 0.0020	0.8552 ± 0.0022	N/A	0.7854 ± 0.0006

Table 2: Comparisons of RMSE against state-of-the-arts on Movielens 100k, 1M, 10M datasets.

Models	Movielens 100K	Models	Movielens 1M	Models	Movielens 10M
ReDa [46]	0.911	NNMF [47]	0.843	GC-MC [48]	0.777
SVD++ [49]	0.913 †	ABCF [50]	0.836	MPMA [51]	0.771
Biased MF [52]	0.911 †	LLoRMA [53]	0.833	CF-NADE [17]	0.771
NNMF [47]	0.907	DMF+ [54]	0.832	SMA [55]	0.768
AutoSVD [56]	0.901	GC-MC [48]	0.832	GLOMA [57]	0.767
DMF+[54]	0.889	AutoRec [16]	0.831	ABCF [50]	0.766
LLoRMA [53]	0.888	CF-NADE [17]	0.829	MRMA [58]	0.763
AutoRec w/SN	0.882	AutoRec w/SN	0.826	AutoRec w/SN	0.769

† : Taken from Zhang et al. [56].

ReLU problem [5]. Setting $K' = n_0$ compensates for the division in SN. We observe the performance is not that sensitive to the value of K' for shallow models or deep models with less than 3 layers³.

Discussion We discuss other forms of SN to alleviate *variable sparsity problem*, already in use unwittingly due to empirical performance improvements.

- The original paper of word2vec [19] proposed to sum up the embedding vectors of several surrounding words, in the CBOW architecture. Later it turns out that using the average operation improves the performance. Since the CBOW model does not include the activation function or bias in the hidden layer, the average at the hidden layer is identical with SN. For the CBOW model, there are differences in the sparsity levels among data instances depending on the number of surrounding words (depending on the locations of words).
- [18] proposed graph convolutional networks for graph-structured data that use an adjacency matrix of graphs as inputs. Applying the normalized graph Laplacian, which is the standard way of representing a graph in graph theory, can naturally handle heterogeneous node degrees and precisely matches the SN operation.
- In the prediction time of Dropout [44], we scale the activations with the drop probability used in the training phase, which might look similar with the SN operation. However, it is instructive to note that the goals of them are orthogonal; the scale of Dropout is fixed across all data instances with diverse sparsity. In fact, we can achieve even better performances by applying both, as shown in the experimental section (Section 5).
- Several works so far have proposed RNN-based models when dealing with sparse data [33, 28, 30, 25]. In the case of vanilla RNNs, the past information disappears rapidly [45] if the standard tanh or sigmoid activations are used, hence the *variable sparsity problem* can be intrinsically suppressed. A similar phenomenon occurs even in RNN variations such as LSTM and GRU. Unlike the vanilla RNN, in LSTM and GRU the past information can survive through gates. If the model is trained properly, the information that survives through the gates will be the information from the informative (probably non-missing) inputs. Therefore, if we build RNN-based models to handle sparse data, it is not that critical to explicitly consider the variable sparsity problem.

³In this paper, we basically use $K' = 1$ for shallow models or deep models with less than 3 layers unless we mention otherwise. However, finding K' via cross-validation might give better results for some models.

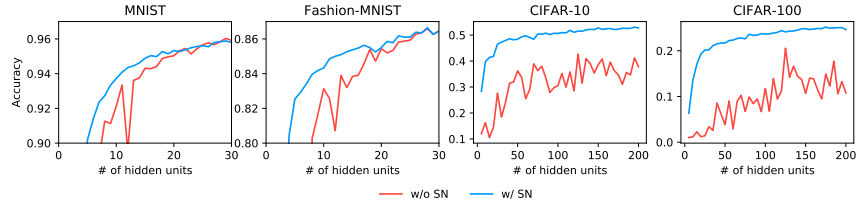


Figure 3: Accuracy of the MLP with and without SN on four benchmark datasets.

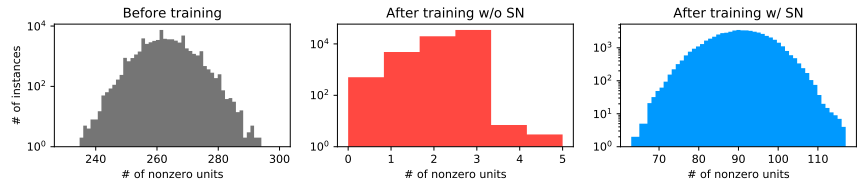


Figure 4: Change of sparsity at the first hidden layer before and after training on CIFAR-10.

5 Experiments

In this section, we evaluate the effect of using SN in 3 different domains⁴. First, we consider neural network-based state-of-the-art models for collaborative filtering which completely ignores the *variable sparsity problem*. Then we tackle inherent missingness from a clinical time-series dataset, with MLP classifiers. Finally, we evaluate SN with MLP classifiers on image datasets such as MNIST [13], Fashion MNIST [14], and CIFAR [15], which have variable sparsity problems but have been overlooked. For fair comparisons, we use Adam optimizer [59] in all experiments. All results are average of 5 runs. In some tables, we also report the standard errors at 95% confidence interval.

Collaborative filtering task First we apply our SN on the collaborative filtering problem. We apply SN to two models, AutoRec [16] and CF-NADE [17] which are state-of-the-arts models among neural-networks-based collaborative filtering methods. Most of the settings including usage of 500 hidden units are followed by original the AutoRec [16] and CF-NADE [17] models (See Appendix D.1). Especially, for CF-NADE, they used weight sharing (WS) and averaging possible choices (APC) in addition to weight decay. We report the results of applying SN without WS or APC. With SN, the models achieve similar or better performance to original CF-NADE model without WS or APC. We use Movielens 100k, Movielens 1M, and, Movielens 10M for these experiments, using randomly selected 10% of the ratings of each datasets for the test set [60]. Since both models can use either of user- or item-rating vector as its input, we report both cases in Table 1. While applying SN clearly improves the performances both in AutoRec and CF-NADE models, the improvement with user-rating is more dramatic. We compare our model (AutoRec with SN) to other states-of-the-arts models⁵. As shown in the Table 2, we achieve states-of-the-arts performance on Movielens 100K and 1M data by simply applying SN to AutoRec. AutoRec with SN outperforms many of the baseline models even on Movielens 10M, and achieve the states-of-the-arts performance among neural-networks-based models⁶. We have tested AutoRec with SN for only a few sets of hyper-parameters. If we tune the hyper-parameters harder, we can get better results.

MLPs on medical datasets We also evaluate SN on five binary classification tasks using health care datasets which have many missing values. The datasets, which is from National Health Insurance Service (NHIS), consists of medical diagnosis of around 300,000 people⁷. Each of datasets has the

⁴In addition to these 3 experiments, additional experiments are given in Appendix C.

⁵For Movielens 1M and 10M, we use 1000 hidden units (See Appendix D.1).

⁶None of SMA [55], GLOMA [57], ABCF [50], and, MRMA [58] is neural-network-based model.

⁷All input data are preprocessed with zero-one normalization.

Table 3: Test AUC on NHIS dataset.

Dataset		Cardiovascular	Fatty Liver	Hypertension	Heart Failure	Diabetes
MLP	w/o SN	0.7057 \pm 0.0027	0.6750 \pm 0.0050	0.7977 \pm 0.0027	0.7834 \pm 0.0036	0.9121 \pm 0.0097
	w/ SN	0.7106 \pm 0.0005	0.6911 \pm 0.0022	0.8096 \pm 0.0010	0.7914 \pm 0.0012	0.9283 \pm 0.0011
MLP+Dropout	w/o SN	0.7084 \pm 0.0005	0.6858 \pm 0.0065	0.8023 \pm 0.0054	0.7876 \pm 0.0012	0.9263 \pm 0.0026
	w/ SN	0.7105 \pm 0.0009	0.6941 \pm 0.0011	0.8086 \pm 0.0016	0.7922 \pm 0.0015	0.9303 \pm 0.0029

target value which indicates the occurrence of specific disease and the goal is to predict the disease occurrence from medical diagnosis information. We train MLPs with two options on Dropout and SN (4 possible cases), and evaluate in terms of AUC. As shown in Table 3, SN technique not only improves the performance over the baseline MLP (without Dropout) on all five datasets, but also gives additional improvement when applied to MLPs with Dropout. In addition, applying SN shows narrow confidence intervals for most cases than the model without SN.

MLPs and CNNs on vision datasets As we have seen in the Figure 1, MNIST, Fashion MNIST, and CIFAR datasets have different sparsity characteristics across data instances. Now, we compare the accuracies of MLPs w/ and w/o SN on these datasets, as we increase the network capacity⁸. As Figure 3 indicated, the model with SN exhibits some improvements or at least comparable performances. Especially, the smaller the capacity, the more outperform SN model is. In particular, SN achieves similar performances with smaller network size.

Table 4: Test accuracy of VGG-16 models with batch normalization or SN on CIFAR-10 datasets.

	VGG-16	VGG-16 + BN
w/o SN	0.8050 \pm 0.0185	0.8755 \pm 0.0066
w/ SN	0.8094 \pm 0.0173	0.8800 \pm 0.0101

Figure 4 shows the histogram of the sparsity of the first hidden layer activation on a CIFAR-10 dataset⁹. If SN is not applied, the first hidden layer becomes extremely sparse after training, which is likely to lead to abnormal training. When applying SN, the statistic of the first hidden layer appears to be relatively stable after training¹⁰.

We also test the effect of SN on CNN models. Toward this, we use VGG-16 model on CIFAR-10¹¹. As can be seen from the experimental results in Table 4, SN improves or remains similar performance, and has an orthogonal effect with batch normalization.

6 Conclusion

We introduced the *variable sparsity problem*, where the representations can have different values due to varying degree of input-level sparsity, which is one of the many difficulties in stabilizing the training of deep neural networks. To tackle the variable sparsity problem, we proposed *Sparsity Normalization (SN)* that will let the same non-zero features to have the same effects regardless of the sparsity level. With several assumptions, we theoretically analyzed that sparsity normalization can solve the *variable sparsity problem*. Further, we performed experiments on diverse datasets with multiple deep network models to show that sparsity normalization obtains significant improvements over models without normalization, or achieve less capacity with similar performance. Notably, we showed that we could achieve extra performance improvements with Batch Normalization and Dropout, two of the most crucial regularization techniques for training deep neural networks, and have achieved state-of-the-art performances on collaborative filtering problem on the MovieLens 100K and 1M datasets.

⁸We use two hidden layers with ReLU activation and Adam optimizer with a learning of 10^{-2} . MNIST datasets are splitted with training:valid:test=5 : 1 : 1, and CIFAR with 4 : 1 : 1.

⁹We use 512 units per each hidden layers.

¹⁰Before training, the sparsity patterns w/ SN and w/o SN are the same. (See Appendix A.5)

¹¹Dataset is splitted with training:valid:test=10 : 1 : 1.

References

- [1] Xavier Glorot, Antoine Bordes, and Yoshua Bengio. Deep sparse rectifier neural networks. In *Proceedings of the fourteenth international conference on artificial intelligence and statistics*, pages 315–323, 2011.
- [2] Karen Simonyan and Andrew Zisserman. Very deep convolutional networks for large-scale image recognition. *arXiv preprint arXiv:1409.1556*, 2014.
- [3] Christian Szegedy, Wei Liu, Yangqing Jia, Pierre Sermanet, Scott Reed, Dragomir Anguelov, Dumitru Erhan, Vincent Vanhoucke, and Andrew Rabinovich. Going deeper with convolutions. In *Proceedings of the IEEE conference on computer vision and pattern recognition*, pages 1–9, 2015.
- [4] Xavier Glorot and Yoshua Bengio. Understanding the difficulty of training deep feedforward neural networks. In *Proceedings of the thirteenth international conference on artificial intelligence and statistics*, pages 249–256, 2010.
- [5] Kaiming He, Xiangyu Zhang, Shaoqing Ren, and Jian Sun. Delving deep into rectifiers: Surpassing human-level performance on imagenet classification. In *Proceedings of the IEEE international conference on computer vision*, pages 1026–1034, 2015.
- [6] Kaiming He, Xiangyu Zhang, Shaoqing Ren, and Jian Sun. Deep residual learning for image recognition. In *Proceedings of the IEEE conference on computer vision and pattern recognition*, pages 770–778, 2016.
- [7] Gao Huang, Zhuang Liu, Laurens Van Der Maaten, and Kilian Q Weinberger. Densely connected convolutional networks. In *Proceedings of the IEEE conference on computer vision and pattern recognition*, pages 4700–4708, 2017.
- [8] Sergey Ioffe and Christian Szegedy. Batch normalization: Accelerating deep network training by reducing internal covariate shift. *arXiv preprint arXiv:1502.03167*, 2015.
- [9] Jimmy Lei Ba, Jamie Ryan Kiros, and Geoffrey E Hinton. Layer normalization. *arXiv preprint arXiv:1607.06450*, 2016.
- [10] Tim Salimans and Durk P Kingma. Weight normalization: A simple reparameterization to accelerate training of deep neural networks. In *Advances in Neural Information Processing Systems*, pages 901–909, 2016.
- [11] Yuxin Wu and Kaiming He. Group normalization. In *Proceedings of the European Conference on Computer Vision (ECCV)*, pages 3–19, 2018.
- [12] Hyeonseob Nam and Hyo-Eun Kim. Batch-instance normalization for adaptively style-invariant neural networks. In *Advances in Neural Information Processing Systems*, pages 2558–2567, 2018.
- [13] Yann LeCun. The mnist database of handwritten digits. <http://yann.lecun.com/exdb/mnist/>, 1998.
- [14] Han Xiao, Kashif Rasul, and Roland Vollgraf. Fashion-mnist: a novel image dataset for benchmarking machine learning algorithms. *arXiv preprint arXiv:1708.07747*, 2017.
- [15] Alex Krizhevsky, Vinod Nair, and Geoffrey Hinton. Cifar-10 and cifar-100 datasets. *URL: https://www.cs.toronto.edu/kriz/cifar.html*, 6, 2009.
- [16] Suvash Sedhain, Aditya Krishna Menon, Scott Sanner, and Lexing Xie. Autorec: Autoencoders meet collaborative filtering. In *Proceedings of the 24th International Conference on World Wide Web*, pages 111–112. ACM, 2015.

- [17] Yin Zheng, Bangsheng Tang, Wenkui Ding, and Hanning Zhou. A neural autoregressive approach to collaborative filtering. *arXiv preprint arXiv:1605.09477*, 2016.
- [18] Thomas N Kipf and Max Welling. Semi-supervised classification with graph convolutional networks. *arXiv preprint arXiv:1609.02907*, 2016.
- [19] Tomas Mikolov, Kai Chen, Greg Corrado, and Jeffrey Dean. Efficient estimation of word representations in vector space. *arXiv preprint arXiv:1301.3781*, 2013.
- [20] Hidetoshi Shimodaira. Improving predictive inference under covariate shift by weighting the log-likelihood function. *Journal of statistical planning and inference*, 90(2):227–244, 2000.
- [21] Jing Jiang. A literature survey on domain adaptation of statistical classifiers.
- [22] Shibani Santurkar, Dimitris Tsipras, Andrew Ilyas, and Aleksander Madry. How does batch normalization help optimization? In *Advances in Neural Information Processing Systems*, pages 2483–2493, 2018.
- [23] Mengye Ren, Renjie Liao, Raquel Urtasun, Fabian H Sinz, and Richard S Zemel. Normalizing the normalizers: Comparing and extending network normalization schemes. *arXiv preprint arXiv:1611.04520*, 2016.
- [24] Volker Tresp, Subutai Ahmad, and Ralph Neuneier. Training neural networks with deficient data. In *Advances in neural information processing systems*, pages 128–135, 1994.
- [25] Zhengping Che, Sanjay Purushotham, Kyunghyun Cho, David Sontag, and Yan Liu. Recurrent neural networks for multivariate time series with missing values. *Scientific reports*, 8(1):6085, 2018.
- [26] Vladimiro Miranda, Jakov Krstulovic, Hrvoje Keko, Cristiano Moreira, and Jorge Pereira. Reconstructing missing data in state estimation with autoencoders. *IEEE Transactions on power systems*, 27(2):604–611, 2011.
- [27] Pierre-Alexandre Mattei and Jes Frellsen. missiwae: Deep generative modelling and imputation of incomplete data. *arXiv preprint arXiv:1812.02633*, 2018.
- [28] Wei Cao, Dong Wang, Jian Li, Hao Zhou, Lei Li, and Yitan Li. Brits: Bidirectional recurrent imputation for time series. In *Advances in Neural Information Processing Systems*, pages 6775–6785, 2018.
- [29] Jinsung Yoon, James Jordon, and Mihaela Van Der Schaar. Gain: Missing data imputation using generative adversarial nets. *arXiv preprint arXiv:1806.02920*, 2018.
- [30] Yonghong Luo, Xiangrui Cai, Ying Zhang, Jun Xu, et al. Multivariate time series imputation with generative adversarial networks. In *Advances in Neural Information Processing Systems*, pages 1596–1607, 2018.
- [31] Pascal Vincent, Hugo Larochelle, Yoshua Bengio, and Pierre-Antoine Manzagol. Extracting and composing robust features with denoising autoencoders. In *Proceedings of the 25th international conference on Machine learning*, pages 1096–1103. ACM, 2008.
- [32] Manzil Zaheer, Satwik Kottur, Siamak Ravanbakhsh, Barnabas Poczos, Ruslan R Salakhutdinov, and Alexander J Smola. Deep sets. In *Advances in neural information processing systems*, pages 3391–3401, 2017.
- [33] Oriol Vinyals, Samy Bengio, and Manjunath Kudlur. Order matters: Sequence to sequence for sets. *arXiv preprint arXiv:1511.06391*, 2015.
- [34] Marek Śmieja, Łukasz Struski, Jacek Tabor, Bartosz Zieliński, and Przemysław Spurek. Processing of missing data by neural networks. In *Advances in Neural Information Processing Systems*, pages 2719–2729, 2018.

- [35] Zachary C Lipton, David C Kale, and Randall Wetzel. Modeling missing data in clinical time series with rnns. *Machine Learning for Healthcare*, 2016.
- [36] Oleksii Kuchaiev and Boris Ginsburg. Training deep autoencoders for collaborative filtering. *arXiv preprint arXiv:1708.01715*, 2017.
- [37] Philip Bachman, Alessandro Sordoni, and Adam Trischler. Learning algorithms for active learning. In *Proceedings of the 34th International Conference on Machine Learning-Volume 70*, pages 301–310. JMLR. org, 2017.
- [38] Xiangnan He, Lizi Liao, Hanwang Zhang, Liqiang Nie, Xia Hu, and Tat-Seng Chua. Neural collaborative filtering. In *Proceedings of the 26th International Conference on World Wide Web*, pages 173–182. International World Wide Web Conferences Steering Committee, 2017.
- [39] Florian Strub and Jeremie Mary. Collaborative filtering with stacked denoising autoencoders and sparse inputs. In *NIPS workshop on machine learning for eCommerce*, 2015.
- [40] Andrew L Maas, Awni Y Hannun, and Andrew Y Ng. Rectifier nonlinearities improve neural network acoustic models. In *Proc. icml*, volume 30, page 3, 2013.
- [41] Djork-Arné Clevert, Thomas Unterthiner, and Sepp Hochreiter. Fast and accurate deep network learning by exponential linear units (elus). *arXiv preprint arXiv:1511.07289*, 2015.
- [42] Charles Dugas, Yoshua Bengio, François Bélisle, Claude Nadeau, and René Garcia. Incorporating second-order functional knowledge for better option pricing. In *Advances in neural information processing systems*, pages 472–478, 2001.
- [43] Fulufhelo V Nelwamondo, Shakir Mohamed, and Tshilidzi Marwala. Missing data: A comparison of neural network and expectation maximization techniques. *Current Science*, pages 1514–1521, 2007.
- [44] Nitish Srivastava, Geoffrey Hinton, Alex Krizhevsky, Ilya Sutskever, and Ruslan Salakhutdinov. Dropout: a simple way to prevent neural networks from overfitting. *The Journal of Machine Learning Research*, 15(1):1929–1958, 2014.
- [45] Yoshua Bengio, Patrice Simard, Paolo Frasconi, et al. Learning long-term dependencies with gradient descent is difficult. *IEEE transactions on neural networks*, 5(2):157–166, 1994.
- [46] Fuzhen Zhuang, Zhiqiang Zhang, Mingda Qian, Chuan Shi, Xing Xie, and Qing He. Representation learning via dual-autoencoder for recommendation. *Neural Networks*, 90:83–89, 2017.
- [47] Gintare Karolina Dziugaite and Daniel M Roy. Neural network matrix factorization. *arXiv preprint arXiv:1511.06443*, 2015.
- [48] Rianne van den Berg, Thomas N Kipf, and Max Welling. Graph convolutional matrix completion. *arXiv preprint arXiv:1706.02263*, 2017.
- [49] Yehuda Koren. Factorization meets the neighborhood: a multifaceted collaborative filtering model. In *Proceedings of the 14th ACM SIGKDD international conference on Knowledge discovery and data mining*, pages 426–434. ACM, 2008.
- [50] Mingsheng Fu, Hong Qu, Dagmawi Moges, and Li Lu. Attention based collaborative filtering. *Neurocomputing*, 311:88–98, 2018.
- [51] Chao Chen, Dongsheng Li, Qin Lv, Junchi Yan, Stephen M Chu, and Li Shang. Mpma: Mixture probabilistic matrix approximation for collaborative filtering.
- [52] Yehuda Koren, Robert Bell, and Chris Volinsky. Matrix factorization techniques for recommender systems. *Computer*, (8):30–37, 2009.

- [53] Joonseok Lee, Seungyeon Kim, Guy Lebanon, Yoram Singer, and Samy Bengio. Llorma: Local low-rank matrix approximation. *The Journal of Machine Learning Research*, 17(1):442–465, 2016.
- [54] Baolin Yi, Xiaoxuan Shen, Hai Liu, Zhaoli Zhang, Wei Zhang, Sannyuya Liu, and Naixue Xiong. Deep matrix factorization with implicit feedback embedding for recommendation system. *IEEE Transactions on Industrial Informatics*, 2019.
- [55] Dongsheng Li, Chao Chen, Qin Lv, Junchi Yan, Li Shang, and Stephen Chu. Low-rank matrix approximation with stability. In *International Conference on Machine Learning*, pages 295–303, 2016.
- [56] Shuai Zhang, Lina Yao, and Xiwei Xu. Autosvd++: An efficient hybrid collaborative filtering model via contractive auto-encoders. In *Proceedings of the 40th International ACM SIGIR conference on Research and Development in Information Retrieval*, pages 957–960. ACM, 2017.
- [57] Chao Chen, Dongsheng Li, Qin Lv, Junchi Yan, Li Shang, and Stephen M Chu. Gloma: Embedding global information in local matrix approximation models for collaborative filtering. In *Thirty-First AAAI Conference on Artificial Intelligence*, 2017.
- [58] Dongsheng Li, Chao Chen, Wei Liu, Tun Lu, Ning Gu, and Stephen Chu. Mixture-rank matrix approximation for collaborative filtering. In *Advances in Neural Information Processing Systems*, pages 477–485, 2017.
- [59] Diederik P Kingma and Jimmy Ba. Adam: A method for stochastic optimization. *arXiv preprint arXiv:1412.6980*, 2014.
- [60] F Maxwell Harper and Joseph A Konstan. The movielens datasets: History and context. *Acm transactions on interactive intelligent systems (tiis)*, 5(4):19, 2016.
- [61] Martín Abadi, Paul Barham, Jianmin Chen, Zhifeng Chen, Andy Davis, Jeffrey Dean, Matthieu Devin, Sanjay Ghemawat, Geoffrey Irving, Michael Isard, et al. Tensorflow: A system for large-scale machine learning. In *12th {USENIX} Symposium on Operating Systems Design and Implementation ({OSDI} 16)*, pages 265–283, 2016.
- [62] Adam Paszke, Sam Gross, Soumith Chintala, and Gregory Chanan. Pytorch: Tensors and dynamic neural networks in python with strong gpu acceleration. *PyTorch: Tensors and dynamic neural networks in Python with strong GPU acceleration*, 6, 2017.

A Proofs

A.1 Proof of Theorem 1

Proof. From the definition of $h_l, w_l^1, h_l^0, \tilde{h}_l^0, m_l$, the following equation holds.

$$E[h_l^1] = n_0 E[w_l^1 h_l^0] = n_0 E[w_l^1 \tilde{h}_l^0 m_l] \quad (2)$$

From the Assumption 1, w_l^1, \tilde{h}_l^0 , and m_l are independent of each other. Thus,

$$E[h_l^1] = n_0 E[w_l^1] E[\tilde{h}_l^0] E[m_l] \quad (3)$$

Similarly, the following holds.

$$E[h_l^i] = n_{i-1} E[w_l^i h_l^{i-1}] \text{ for } i = 1, \dots, L \quad (4)$$

Since h_l^{i-1} and w_l^i are independent of each other by the Assumption 1 and the definition of h_l^{i-1} , $E[h_l^i] = n_{i-1} E[w_l^i] E[h_l^{i-1}]$. Therefore,

$$E[h_l^L] = \prod_{i=1}^L n_{i-1} E[w_l^i] E[\tilde{h}_l^0] E[m_l] = \prod_{i=1}^L n_{i-1} \mu_w^i \mu_x \mu_m \quad (5)$$

□

A.2 Proof of Theorem 2

Proof. From the definition of $h_l, w_l^1, h_l^0, \tilde{h}_l^0, m_l$ and the property of an affine function $\sigma(E[\cdot]) = E[\sigma(\cdot)]$, the following equation holds.

$$E[h_l^1] = \sigma(n_0 E[w_l^1 h_l^0] + E[b_l^1]) = \sigma(n_0 E[w_l^1 \tilde{h}_l^0 m_l] + E[b_l^1]) \quad (6)$$

From the Assumption 1, w_l^1, \tilde{h}_l^0 , and m_l are independent of each other. Thus,

$$E[h_l^1] = \sigma(n_0 E[w_l^1] E[\tilde{h}_l^0] E[m_l] + E[b_l^1]) \quad (7)$$

$$= \sigma(n_0 \mu_w^1 \mu_x \mu_m + \mu_b^1) \quad (8)$$

$$= f_1(\mu_x \mu_m) \quad (9)$$

Similarly, the following holds.

$$E[h_l^i] = \sigma(n_{i-1} E[w_l^i h_l^{i-1}] + E[b_l^i]) \text{ for } i = 1, \dots, L \quad (10)$$

Since h_l^{i-1} and w_l^i are independent of each other by the Assumption 1 and the definition of h_l^{i-1} ,

$$E[h_l^i] = \sigma(n_{i-1} E[w_l^i] E[h_l^{i-1}] + E[b_l^i]) \quad (11)$$

$$= \sigma(n_{i-1} \mu_w^i E[h_l^{i-1}] + \mu_b^i) \quad (12)$$

$$= f_i(E[h_l^{i-1}]) \quad (13)$$

Therefore,

$$E[h_l^L] = f_L \circ \dots \circ f_1(\mu_x \mu_m) \quad (14)$$

□

A.3 Proof of Theorem 3

Proof. From the definition of $h_l, w_l^1, h_l^0, \tilde{h}_l^0, m_l$ and the property of a convex function $E[\sigma(\cdot)] \geq \sigma(E[\cdot])$, the following equation holds.

$$E[h_l^1] \geq \sigma(n_0 E[w_l^1 h_l^0] + E[b_l^1]) = \sigma(n_0 E[w_l^1 \tilde{h}_l^0 m_l] + E[b_l^1]) \quad (15)$$

From the Assumption 1, w_l^1 , \tilde{h}_l^0 , and m_l are independent of each other. Thus,

$$E[h_l^1] \geq \sigma \left(n_0 E[w_l^1] E[\tilde{h}_l^0] E[m_l] + E[b_l^1] \right) \quad (16)$$

$$= \sigma \left(n_0 \mu_w^1 \mu_x \mu_m + \mu_b^1 \right) \quad (17)$$

$$= f_1(\mu_x \mu_m) \quad (18)$$

Similarly, the following holds.

$$E[h_l^i] \geq \sigma \left(n_{i-1} E[w_l^i h_l^{i-1}] + E[b_l^i] \right) \text{ for } i = 1, \dots, L \quad (19)$$

Since h_l^{i-1} and w_l^i are independent of each other by the Assumption 1 and the definition of h_l^{i-1} ,

$$E[h_l^i] \geq \sigma \left(n_{i-1} E[w_l^i] E[h_l^{i-1}] + E[b_l^i] \right) \quad (20)$$

$$= \sigma \left(n_{i-1} \mu_w^i E[h_l^{i-1}] + \mu_b^i \right) \quad (21)$$

$$= f_i(E[h_l^{i-1}]) \quad (22)$$

Therefore,

$$E[h_l^L] \geq f_L \circ \dots \circ f_1(\mu_x \mu_m) \quad (23)$$

□

A.4 Proof of Theorem 4

Proof. By theorem 2, $E[h_l^L] = f_L \circ \dots \circ f_1(E[\mathbf{h}_{\text{SN}}^0])$. Since $E[\mathbf{h}_{\text{SN}}^0] = E[\mathbf{h}^0] \cdot K/\mu_m$,

$$E[h_l^L] = f_L \circ \dots \circ f_1(\mu_x \mu_m \cdot K/\mu_m) = f_L \circ \dots \circ f_1(\mu_x \cdot K) \quad (24)$$

□

A.5 Why are the Sparsity Patterns Same Before Training?

In Section 5, we show how the sparsity of the activation of the first hidden layer changes when SN is applied and when it is not on the CIFAR-10 dataset. And, we claim that the differences of sparsity in first hidden layer between data instances with SN and without SN are the same before training.

Proof. Because, we use ReLU activation and zero initialized bias:

$$\sum_l \mathbb{I}(\sigma(W^1 \mathbf{h}^0 + \mathbf{b}^1)_l \neq 0) \quad (25)$$

$$= \sum_l \mathbb{I}(\sigma(W^1 \mathbf{h}^0)_l \neq 0) \quad (26)$$

$$= \sum_l \mathbb{I}((W^1 \mathbf{h}^0)_l > 0) \quad (27)$$

$$= \sum_l \mathbb{I}((W^1 \mathbf{h}^0 / \|\mathbf{h}^0\|_0)_l > 0) \quad (28)$$

$$= \sum_l \mathbb{I}(\sigma(W^1 \mathbf{h}^0 / \|\mathbf{h}^0\|_0)_l \neq 0) \quad (29)$$

□

B Sparsity Normalization for CNN

The SN techniques presented in this paper are generic techniques that do not depend on a particular model. In this subsection, we present how to apply SN to a CNN architecture. In particular, because CNN performs zero-padding, sparsity occurs even if sparsity does not exist in the image data. Therefore, SN may have a beneficial effect on CNN training. Typical differences between CNN and MLP are the dimensions of the input and hidden layers. In MLP, the input layer can be expressed as a vector, whereas in a CNN it must be represented as a matrix. If the first hidden layer of the CNN is H^1 and the input layer is H^0 , we can determine the first hidden layer from the input layer, as in the MLP, as follows.

$$H^1 = \sigma(W^1 H^0 + \mathbf{b} \mathbf{1}_{n_0}^T) \quad (30)$$

Let the filter size be k , the input image channel c , and the first hidden layer channel d , then we can then obtain $H^1 \in \mathbb{R}^{d \times n_0}$, $W^1 \in \mathbb{R}^{d \times k^2 c}$, $H^0 \in \mathbb{R}^{k^2 c \times n_0}$, $\mathbf{1}_{n_0} \in \mathbb{R}^{n_0}$, $\mathbf{b} \in \mathbb{R}^d$. If we write a column vector of H^0 as \mathbf{h}^0 and write a column vector of H^1 as \mathbf{h}^1 , we can rewrite the expression as follows:

$$\mathbf{h}^1 = \sigma(W^1 \mathbf{h}^0 + \mathbf{b}) \quad (31)$$

Similar to the process of applying SN in MLP networks, when $W^1 \mathbf{h}^0$ is independent of the sparsity of \mathbf{h}^0 , \mathbf{h}^1 becomes independent of the sparsity of \mathbf{h}^0 , and output activation becomes independent of the sparsity of \mathbf{h}^0 eventually. Therefore, to apply SN to a CNN, we change \mathbf{h}^1 to \mathbf{h}_{SN}^1 as follows.

$$\mathbf{h}_{\text{SN}}^1 = \sigma \left(W^1 \frac{\mathbf{h}^0}{\|\mathbf{h}^0\|_0} + \mathbf{b} \right) \quad (32)$$

As indicated in (32) and in Theorem 4, SN for CNN is quite similar to the SN for the MLP. It is easy to observe that these operations can be implemented without modifying the internals of the convolution functions provided in widely used deep learning frameworks such as tensorflow [61] or pytorch [62] (See Algorithm 2).

Algorithm 2 Sparsity Normalized Convolutional Layer (Conv_{SN})

Input: Convolutional layer $\text{Conv}(\mathbf{x})$ without non-linearity, learnable bias \mathbf{b} .

Output: Sparsity normalized convolutional layer $\text{Conv}_{\text{SN}}(\mathbf{x})$.

Remove bias of $\text{Conv}(\mathbf{x})$

$\text{Conv}_{\text{divider}}(\mathbf{x}) \leftarrow \text{Deep copy of } \text{Conv}(\mathbf{x})$

Make $\text{Conv}_{\text{divider}}(\mathbf{x})$ non-learnable and set its filter parameter to 1.

$\text{Conv}_{\text{SN}}(\mathbf{x}) \leftarrow \text{Conv}(\mathbf{x}) / \text{Conv}_{\text{divider}}(\|\mathbf{x}\|_0) + \mathbf{b} \mathbf{1}_{n_0}^T$

C Additional Experiments

C.1 Experiments on UCI Datasets

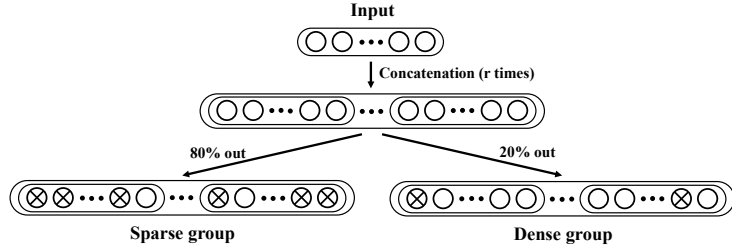


Figure 5: Illustration of manipulating UCI datasets to make sparse and dense groups.

In subsection 3.2, we confirm that there is a *variable sparsity problem* using UCI datasets. In this subsection, we see what happens when SN is applied in the same setting of subsection 3.2 including the sparsity injection process (See Figure 5). We check the effect of SN on 6 UCI datasets (3 classification tasks, 3 regression tasks), including two datasets used in the subsection 3.2. Because we want to use the highly representative UCI datasets, we choose 6 of the UCI datasets that are built into the scikit-learn package, which is widely used for machine learning tasks. Note that all the input data are pre-processed with zero-one normalization.

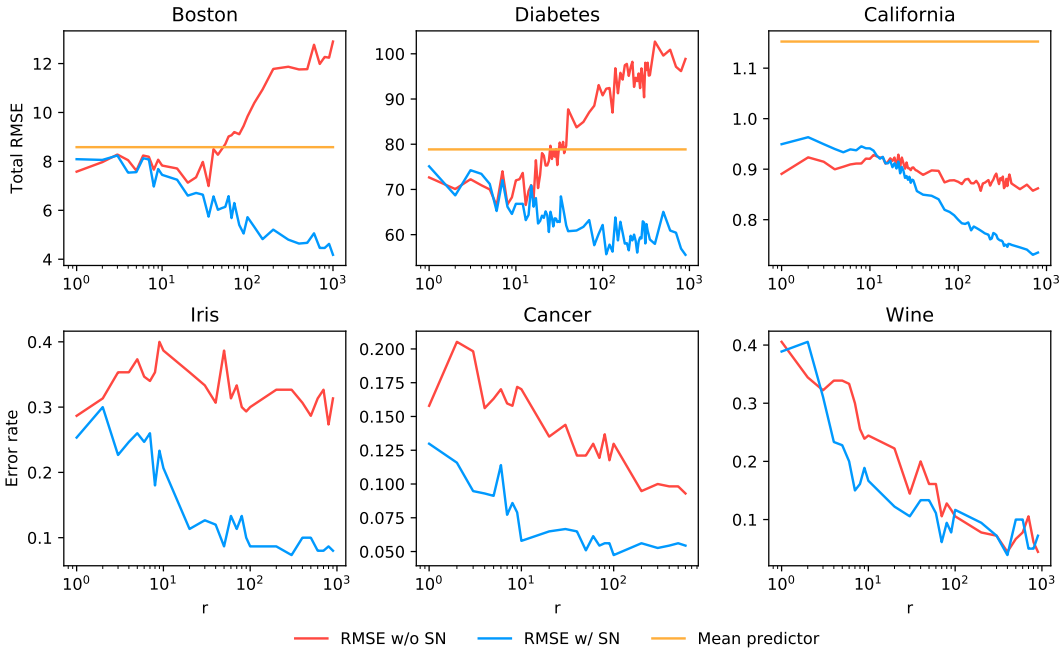


Figure 6: Comparison of the error on the UCI Dataset w/ and w/o SN.

As can be seen in the Figure 6, applying SN for regression tasks, we can see that the error (RMSE, 1 - accuracy) reduces as r increases (information increases). When applying SN for 6 tasks, performance are similar to or better than the model without SN. Figure 7 indicates the expected outputs of each networks of sparse group and dense group with or without SN. For the classification task, the dimension of output layer is larger than 1. In the case of the model without SN for all 6 tasks, there is a quite big difference in the average value of the output layer activations of the dense group and the sparse group, whereas in the case of the model using SN, there is a few difference in the outputs between two groups.

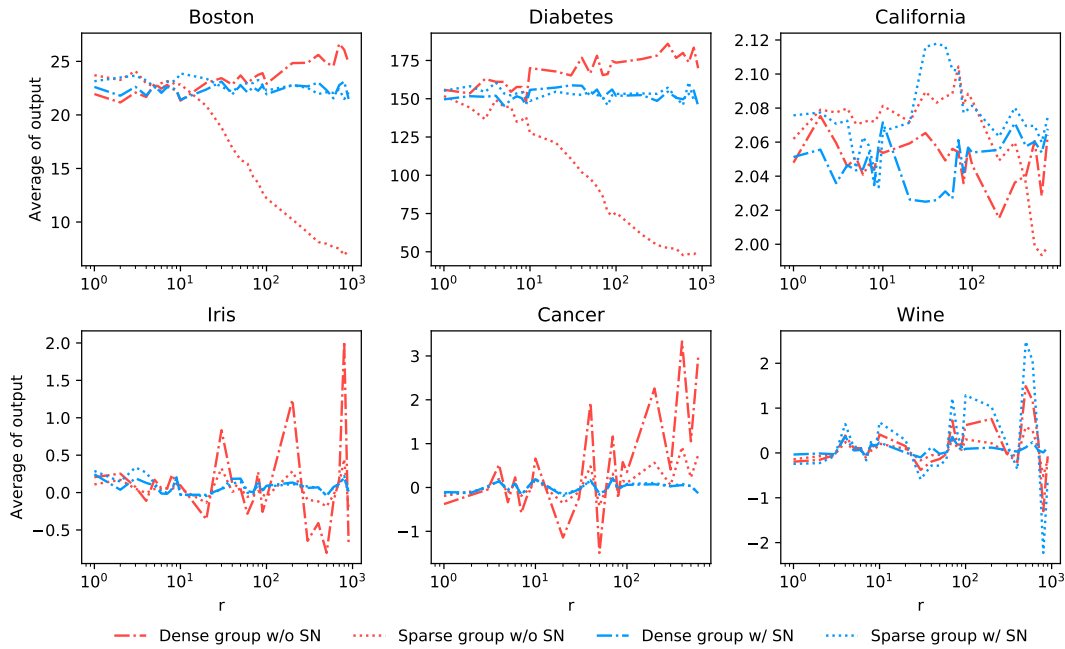


Figure 7: Comparison of the expected output activation on the UCI Dataset w/ and w/o SN.

For the regression tasks presented in the subsection 3.2, the training process is completely broken without SN. However, in the case of the classification tasks, we can't find such phenomenon that training is collapsed. In the case of classification tasks, softmax is used for the back propagation. In this process, it is assumed that this phenomenon is relatively reduced as the output layer is forcibly normalized by softmax function. Nevertheless, for most classification tasks we test, models with SN showed a much lower error rate (less than half).

C.2 Comparisons to Other Simple Missing Handling Methods

We compare our normalization technique SN with other simple missing handling methods in this subsection. Unlike [26, 27, 28, 29, 31, 32, 33, 34], we do not use additional networks nor network parameters. Thus, we only compare our models with missing handling techniques that do not use additional network structures. The models that we set as baseline are as follows.

- **Zero imputation:** The method see missing as zero. It can be seen as a primitive model that does not handle missing at all.
- **Mean imputation:** Missing handling method to impute missing entries to the mean value of each feature.
- **Observation indicator:** A missing handling technique that allows the network to recognize and learn the missingness by itself by concatenating input vector and the mask vector indicating observation or missing. There is a disadvantage that the input dimension doubles and the network capacity of the first layer doubles. The mask vector indicates the observed entry as 1 and the missing entry as 0.
- **Missing indicator:** In contrast to the observation indicator method, the mask vector indicates the observed entry as 0 and the missing entry as 1. This method is suggested by [35, 25].

We use the same 6 UCI datasets as those used in the Appendix C.1, and fixed the r value for the number of replications to 100. The situation with $r = 100$ is that the *variable sparsity problem* appears in most datasets, as you can see in the Figure 7. We see how each missing handling technique can handle the missing in these settings. Since the two indicator methods doubles the input dimension, comparing these methods with our method might not be a fair comparison. However, we have seen that our models can achieve competitive results, even though the indicator methods increase the network capacity of the first layer by a factor of two. The experimental results are summarized in Table 5. RMSE is reported for regression tasks, and classification error is reported for classification tasks. As the Table 5 indicates, sparsity normalization outperforms other missing handling methods in most datasets except California dataset, and sparsity normalization shows lower error with large margin compared to other methods.

Table 5: Comparisons to other simple missing handling techniques to SN

	Boston	Diabetes	California	Iris	Cancer	Wine
Zero imputation	9.782 ± 1.627	98.785 ± 17.674	0.8772 ± 0.0169	0.3200 ± 0.0745	0.1140 ± 0.0557	0.1278 ± 0.1129
Mean imputation	6.058 ± 1.938	63.313 ± 6.947	0.7439 ± 0.0577	0.3333 ± 0.2654	0.1351 ± 0.2018	0.2222 ± 0.2639
Observation indicator	11.253 ± 2.062	105.197 ± 16.793	0.9109 ± 0.0354	0.2867 ± 0.2291	0.0772 ± 0.0477	0.1778 ± 0.1747
Missing indicator	5.864 ± 1.061	65.090 ± 9.874	0.8249 ± 0.0294	0.3467 ± 0.0991	0.1140 ± 0.0544	0.2111 ± 0.1747
Sparsity normalization	5.152 ± 1.271	60.418 ± 7.881	0.8014 ± 0.0141	0.1133 ± 0.0584	0.0491 ± 0.0552	0.0889 ± 0.1116

Performance comparison with existence of variable sparsity problem Among the five methods that have been compared, zero imputation and observation indicators can experience *variable sparsity problem*. We have already seen a variable sparsity problem for zero imputation. Similar to zero imputation, variable sparsity problem can also occur in an observation indicator method, in which the ℓ_0 norm of each data instance is all different. Since the mean imputation makes the entire data set dense, the variable sparsity problem does not occur. In the case of the missing indicator method, the variable sparsity problem does not occur because the missing is treated as 1 and the observation is treated as 0, so that the sparsity is kept the same for each data instance. In this paragraph, we identify performance differences depending on the existence of a variable sparsity problem. Two of the five worst performing models are zero imputation and observation indicators. Even the two models differ in performance from the other models with large margin. This phenomenon is by no means a coincidence, and we diagnose the cause as variable sparsity problem. Although the missing indicator and the observation indicator are quite similar, there is a significant performance difference depending on whether a variable sparsity problem occurs. Even though the observation indicator

method doubles the network capacity of the first layer, it shows a high error because the variable sparsity problem occurs.

Performance comparison with Mean imputation and Missing indicator Since the mean imputation and missing indicators are a way to keep the sparsity level of each input data instance constant, a variable sparsity problem is unlikely to occur. Nonetheless, SN shows the result of outperforming the two models. We explain this phenomenon in this paragraph. Mean imputation does not take into account the characteristics of each data instance and considers the unknown value as an average. In this way, the variable sparsity problem may not occur, but it can be dangerous as [24, 25] have already suggested, since missing is filled without taking into account each data instance characteristic. Similar to the observation indicator, the mask vector compensates for missing equally without considering the characteristics of each data instance. Therefore, it is likely that each data instance property result in less consideration. However, if sparsity normalization is applied, the characteristics of the data instance can be considered sufficiently because the model learns to make decisions only with observed entries. And, consideration of each data instance characteristic results in a performance difference.

C.3 Sparsity Normalization in Hidden Layer

In this paper, we have only discussed how to apply Sparsity Normalization to the input layer. At this subsection, a very natural question is whether sparsity normalization is effective in a hidden layer. Since a hidden layer can be regarded as the input layer of the upper network, there is a possibility that the sparsity normalization is effective in a hidden layer. Heterogeneity of sparsity can occur frequently in a hidden layer because of ReLU or dropout inducing sparsity in a hidden layer.

Unfortunately, applying sparsity normalization to the hidden layer is not that simple. To apply sparsity normalization, the ℓ_0 norm of hidden layer activation must be calculated. Hidden layer activation is parameterized to the network weight. When normalization is performed by calculating ℓ_0 norm, the gradient of ℓ_0 norm should be calculated. However, as is well known, ℓ_0 norm has difficulty in calculating the gradient, which can lead to unstable learning. Therefore, we need to solve it in a different way.

To solve the difficulty in calculating gradient of ℓ_0 norm, ℓ_1 norm may be used instead, or stochastic calculation using hard sigmoid may be used. Among the various possible methods, we decide to look at the ℓ_0 norm as a constant, which does not calculate gradient for the norm, to simply check the possibility of applying sparsity normalization to a hidden layer. We decide to explore further on the other possible options later in future works.

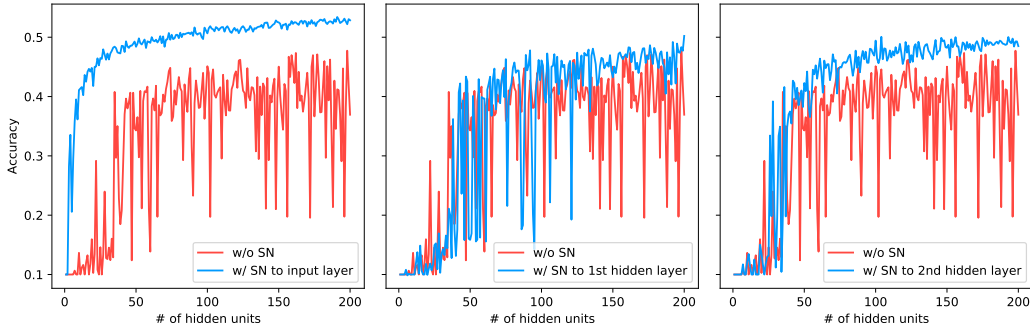


Figure 8: The accuracy applying SN to input layer, 1st hidden layer, and 2nd hidden layer on CIFAR-10

We perform the same experiment as the vision MLP experiment presented in Section 5 on the CIFAR-10 dataset. Unfortunately, because of the time constraint, the experiments in this section are performed only once. Figure 8 shows the results of applying the SN to the input layer, the first hidden layer, and the second hidden layer. It is most effective when applied to the input layer, but it is difficult to compare simply because the method of applying the SN to the hidden layer is not a straight forward method. Note that sparsity normalization can be applied to the hidden layer. And Figure 9 compares the result of applying SN only to input layer and additionally applied first hidden layer. There is no big difference in performance. Similar to batch normalization, the internal statistic needs a slightly deeper network to change, but it seems to have not seen a big difference because it uses a network with only two hidden layers. It will be necessary to verify the effect of the SN through experiments to apply the SN to a hidden layer of deeper network in the future works.

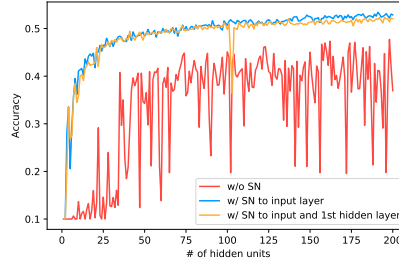


Figure 9: The accuracy applying SN only to input layer, and additionally applied first hidden layer on CIFAR-10

C.4 Why we use Adam Optimizer in AutoRec?

In this subsection we explain why we use Adam Optimizer to train the AutoRec model. The authors of AutoRec used an optimizer called Resilient Propagation (RProp) to train the AutoRec model. This optimizer has a fast convergence speed but can only be used in full batch. When training MovieLens 10M data using AutoRec based on item vector, training in full batch is not possible with 12GB of GPU memory. So, we decide to use Adam Optimizer. However, the performance of Adam should not be lower than that of RProp. Fortunately, we find that using Adam in most cases show similar or better performance to using RProp. The experimental results are summarized in Table 6.

Table 6: Test RMSE on MovieLens 100k, 1M, 10M datasets using Adam and RProp.

Datasets	MovieLens 100k		MovieLens 1M		MovieLens 10M	
	item vector	user vector	item vector	user vector	item vector	user vector
RProp	0.8861	0.9437	0.8358	0.8804	0.782 [†]	0.867[†]
Adam	0.8831	0.9343	0.8306	0.8832	0.7807	0.8859

[†] : Taken from Sedhain et al. [16].

C.5 Why 500 hidden units are not sufficient on AutoRec with SN?

[16] say 500 hidden layers are sufficient for AutoRec. But we think that it requires more network capacity at least in the case of applying SN. The Figure 10 plots the test RMSE, changing the number of hidden units for MovieLens 100k and 1M. We can see that 600 units for MovieLens 100k and 900 units for MovieLens 1M are necessary for getting better performance. Obviously, as datasets become more complex and larger, we need more network capacity. This is why we use 1000 hidden units for a relatively large MovieLens 1m, 10m datasets on comparing to other states-of-the-arts models. (MovieLens 10m may require larger capacity.)

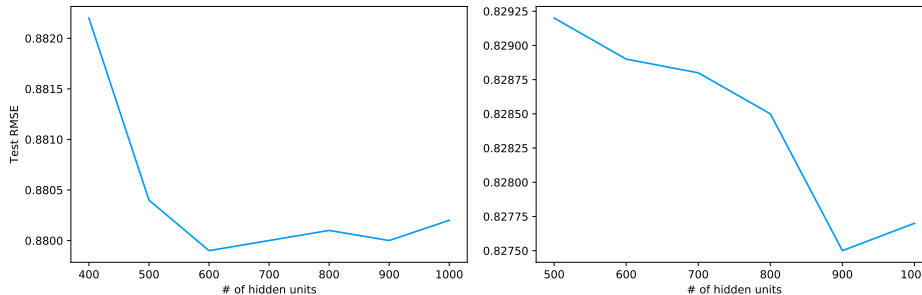


Figure 10: The test RMSE for the number of hidden units when applying SN

C.6 $K' = 1$ in AutoRec and CF-NADE model.

Unlike $K' = 1$ in most other models, we use $K' = n_1$ exceptionally in the collaborative filtering task. The reason is explained in Appendix D.1. When using weight decay, if there is a power imbalance between W^1 and W^2 , the regularization is not properly performed. However, as we have already mentioned, any constant K' can prevent variable sparsity problem. In this subsection, we investigate whether the variable sparsity problem can be prevented even when $K' = 1$ is used.

Before the discussion, we should set the notations for this. First look at how to use a general way to use weight decay for a single hidden layer case. Let \mathcal{L} be a loss function that does not include any regularization, and a new loss function \mathcal{L}' including weight decay can be expressed as:

$$\mathcal{L}' := \mathcal{L} + \lambda (\|W^1\|_F + \|W^2\|_F) \quad (33)$$

where λ is the regularization term for weight decay and $\|\cdot\|_F$ means Frobenius norm of matrix. If we use $K' = 1$ while using SN, the amplitude imbalance between W^1 and W^2 can be large, so we decide to use a new method that uses weight decay only for W^2 .

$$\mathcal{L}'_{\text{SN with } K'=1} := \mathcal{L} + \lambda \|W^2\|_F \quad (34)$$

(Of course, using different lambda values for each W^i may be one way, but in that case, simple comparison with existing models becomes difficult.) The results of training the AutoRec model using this new weight decay are summarized in the Table 7. The experimental results presented in this table are better than the experimental results we presented in Section 5. The reason we do not present these good experimental results in Section 5 is that we decide that the method of weight decay only in W^2 is unfair for comparison. We decide that it would be better to use $K' = n_1$ to compare more objectively the effect of SN in Section 5.

Table 7: Test RMSE of AutoRec on Movielens 100k, 1M, 10M datasets using $K' = 1$.

Datasets	Movielens 100k		Movielens 1M		Movielens 10M	
	item vector	user vector	item vector	user vector	item vector	user vector
w/o SN	0.8831	0.9343	0.8306	0.8832	0.7807	0.8859
w/ SN	0.8798	0.9266	0.8271	0.8581	0.7711	0.8241

Someone might argue that this performance improvement is due to using weight decay only for W^2 . Therefore, we test the effect of SN under the condition of using weight decay only for W^2 . The experimental results are summarized in Table 8. Using weight decay only for W^2 show similar performance compared to the original AutoRec model. And, except for one case, the experimental results of the model with SN is better than the model without SN.

Table 8: Test RMSE of AutoRec on Movielens 100k, 1M, 10M datasets using $K' = 1$ and weight decay only on W^2 .

Datasets	Movielens 100k		Movielens 1M		Movielens 10M	
	item vector	user vector	item vector	user vector	item vector	user vector
w/o SN	0.8838	0.9171	0.8365	0.8612	0.7915	0.8564
w/ SN	0.8798	0.9266	0.8271	0.8581	0.7711	0.8241

In the CF-NADE model, we do a similar experiment on the Movielens 100k dataset, and we are able to get results that show a similar pattern to that of AutoRec.

D Detailed Experimental Settings

D.1 Collaborative Filtering Task

This subsection describes the experimental setting of a detailed collaborative filtering task in Section 5. As already mentioned, we follow the setting of AutoRec, CF-NADE as much as possible. We train neural networks with a single hidden layer with 500 units, with the weight decay regularization. For fair comparisons, we tune the hyper-parameters for weight decay in all experiments to have only one significant digit, and use a learning rate of 10^{-3} for both models¹², except for the AutoRec on Movielens 10M where we used a learning rate of 10^{-4} . We use full batch for AutoRec on Movielens 100k and 1M, mini-batch (1000) for AutoRec on Movielens 10M, and mini-batch (512) for CF-NADE models. We use $K' = n_1$ for all collaborative filtering experiments. Although we have already stated that the choice of K is not sensitive to performance, we note that the use of weight decay as a regularization is an exceptional situation. When using weight decay, the power balance between W^1 and W^2 is heavily important. To balance two weight matrices, we should use $K' = n_1$.

In comparison with other states-of-the-arts models, we used 1000 hidden units in AutoRec [16] with SN. While [16] claimed that they were able to achieve enough performance only with 500 hidden units, 500 hidden units did not achieve sufficient performance when applying SN (See Appendix C.5). Therefore, we decide to use larger network capacity (1000 hidden units) for larger data sets like Movielens 1M and 10M to get better performance. The number of hidden units can also be viewed and tuned as a hyper-parameter, and we have not tuned much for the number of hidden units. We would get better results if we tune this hyper-parameter harder.

D.2 Description of the Machine in the Experiments

We hope our model being widely applicable. As explained in the Section 4, our model can be implemented simply by pre-processing the input data. Therefore, additional resources are unnecessary to apply our model. We perform all the experiments on a Titan X with 12GB of VRAM. 12 GB of VRAM is not always necessary, and most experiments require smaller VRAM. Except for experiments related to the Movielens 10M, all experiments usually complete within three hours.

¹²The original CF-NADE uses learning rate 0.0005 for Movielens 10M, but we use 10^{-3} . Therefore, the results can be somewhat different from original paper.